First International Symposium on Marine Propulsors
smp'09, Trondheim, Norway, June 2009

Advanced Design of a Ducted Propeller with High Bollard Pull Performance

Tadashi Taketani[1], Koyu Kimura[1], Norio Ishii[1], Masao Matsuura[2], Yuichi Tamura[2]

[1]Akishima Laboratories (MITSUI ZOSEN) Inc., Tokyo, Japan
[2]Niigata Power Systems Co., Ltd., Tokyo, Japan

ABSTRACT

A ducted propeller is well known to offer significant advantages for bollard pull performance of tugboats. A study about nozzle and propeller shape has been done for a long time, and a Ka series propeller and a conventional 19A nozzle is used ordinarily for a ducted propeller. In late years a demand of the energy saving becomes very high because of a remarkable rises of the fuel oil price, and high bollard pull performance are demanded for tugboats at the same horsepower. Therefore, an improved design of a ducted propeller with high bollard pull performance is required.

This present paper will describe the advanced design method of a ducted propeller which has high bollard pull performance. A nozzle section shape and a propeller are newly designed by a parametric study of the numerical simulation to have higher performance than a conventional ducted propeller. And the optimum arrangement between nozzle and propeller combination is studied. In order to confirm high bollard pull performance of the improved ducted propeller, the open water tests are carried out in a towing tank of Akishima Lavoratories (MITSUI ZOSEN) Inc. After the evaluation of the test results, the ducted propeller with high bollard pull performance is designed for actual tugboat.

The newly designed ducted propeller is equipped for "Z-peller" of Niigata Power Systems Co., Ltd as a propulsor of a tugboat, and the full-scale bollard pull test is conducted in the actual field. This paper will also present the field test results showing a higher bollard pull performance than the conventional ducted propeller.

Keywords

Ducted propeller, Design method, Bollard pull, CFD, Z-peller

1 INTRODUCTION

Ducted propellers are classified into two types: the cruising type (free-running type) for transport vessels and high-power types for ocean tugboats. Conventional ducted propellers have ordinarily composed of a 19A nozzle and Kaplan propeller. However, in recent years, market demands exceed the performance of the ducted propellers based on this conventional composition.

Demand for high-power ducted propellers with high bollard pull performance continues to rise year after year, spurring improvements in performance. In response to this demand, we developed the advanced high-power type ducted propeller with high bollard pull performance. This paper finally presents that the performance of newly designed ducted propeller was evaluated by full-scale test results and led to successful commercialization of this new type of ducted propeller.

2 Design of Ducted Propeller

The target in this paper was to develop a new 'Z-peller', which is a mainstay product of Niigata Power Systems Co. Ltd, by improving the bollard pull performance of the existing one. Table 1 gives target design conditions.

Table 1 Design Condition

Engine Output		Propeller		Bollard Pull Thrust
[kW]	[RPM]	Dia [m]	[RPM]	[ton]
2206	750	2.7	219.6	over 80.0 at twin

The following three aspects were investigated to develop a new ducted propeller:

- Nozzle shape
- Propeller shape
- Interaction between the nozzle and the propeller

2.1 Nozzle Shape Design

To develop a new nozzle with bollard pull performance exceeding conventional nozzles (19A), we investigated the 19A-based nozzle shape, in particular the parameters of camber and thickness distributions in the nozzle fore/aft part. In addition to nozzle performance, easy manufacturing was considered. We used both theoretical and computational fluid dynamics (CFD) calculations to analyze various shapes. The theoretical method is preferable for parametric studies for shape analysis because it could reduce the time required for calculations.

We used to theoretical calculation based on the Vortex Lattice Method (VLM), often used to calculate propeller characteristics, applying it to explore new nozzle shapes. We evaluated nozzle thrust per unit of propeller thrust (KTD/KTP), comparing this aspect to performance provided by conventional nozzles. KTP and KTD are defined respectively by equation (1) and (2).

$$KTP = \frac{TP}{\rho \cdot n^2 \cdot D^4} \quad (1)$$

$$KTD = \frac{TD}{\rho \cdot n^2 \cdot D^4} \quad (2)$$

Where KTP = propeller thrust coefficient; KTD = nozzle thrust coefficient; TP = propeller thrust; TD = nozzle thrust; ρ = density of water; n = propeller revolution number; D = propeller diameter.

Since the theoretical method is not available for detailed evaluations of flow near the nozzle, we used CFD at the final stage to perform detailed performance evaluations. We used commercial finite-volume code STAR-CD Ver.3.26 fluid analysis software for CFD analysis with a simplified two-dimensional axially symmetric model that provides propeller thrust as the body force. An even thrust inside the nozzle was provided as the body force. The calculation conditions are shown in Table 2. The generated meshes for the calculation are shown in Figure 1. Figure 2 shows the shape of the newly-designed nozzle.

Table 2 Calculation Condition for 2D Analysis

Analysis Solution	2D Steady-State SIMPLE method
Discrete Scheme	QUICK
Turbulence Model	k-ω SST High-Reynolds Number model
Reynolds number	Rn = 6×10^5
Generated meshes	Approx. 45,000 cells (hybrid mesh)

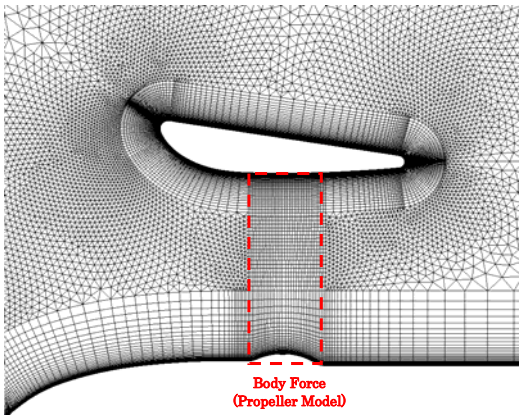

Figure 1 Calculation Meshes for 2D Analysis

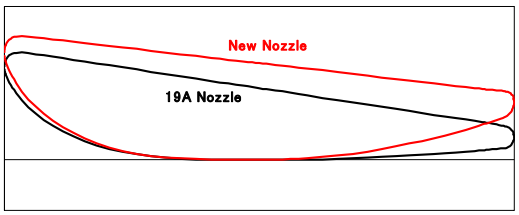

Figure 2 New Designed Nozzle Shape

Figure 3 compares CFD calculations (of the bollard pull condition) for the conventional nozzle and the new nozzle, confirming higher negative pressure at the fore part of new nozzle. Since the nose height of new nozzle is greater than the 19A nozzle, the pressure-receiving area is larger and nozzle thrust is also larger. This results in an approximate improvement of 3.0% for KTD/KTP over the conventional type.

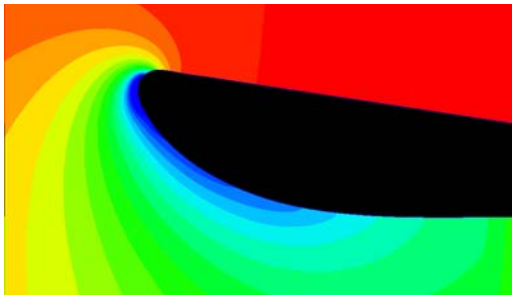

Conventional Nozzle (19A)

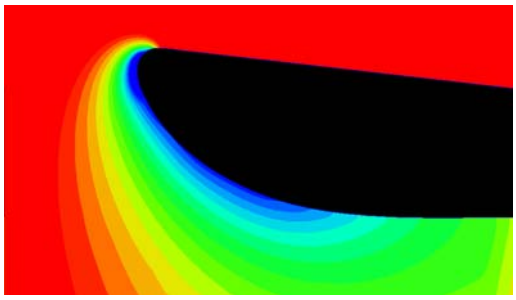

New Designed Nozzle

Figure 3 Comparison of Pressure Distribution

2.2 Propeller Shape Design

Propeller shape is another aspect that should be investigated to achieve high performance in a ducted propeller. For higher performance of the propeller itself, not only the wing-section of the propeller, but also its profile (width/skew distributions) and pitch distribution should be investigated.

For open propellers of several vessels, the NACA wing-section was adopted to improve propeller performance. This wing section also offers advantages over conventional Kaplan propellers with respect to cavitation performance. By selecting a skew distribution to improve

cavitation performance, we can prevent the appearance of bad cavitation. With respect to propeller width distribution, an effective approach is to widen the propeller tip area to increase interaction between the nozzle and the propeller. In this study, based on extensive experience, we selected a skewed Kaplan type profile as the standard shape of the Z-peller, without the problem in cavitation performance, and the propeller wing section was changed to NACA wing section.

Next studied was pitch distribution. For ducted propellers, in contrast to open propellers, the ideal shape is one that provides the highest accelerated inflow into nozzle to maximize nozzle thrust. The key to higher performance of ducted propeller is to accelerate propeller-induced velocity in the area close to the nozzle.

We investigated 2 type pitch distributions (Figure 4) differing in propeller-tip loads which are introduced to evaluate changes in propeller performance with respect to changes in induced velocity by using theoretical and CFD calculations. We used the newly-developed nozzle described in the previous section for evaluation of propeller shape, setting the propeller so that the propeller generator line aligned with the center of the nozzle. The mean pitch ratio was selected so that the same propeller thrust value on the bollard pull condition was calculated by the VLM-based theoretical calculations for each propeller operating inside the nozzle.

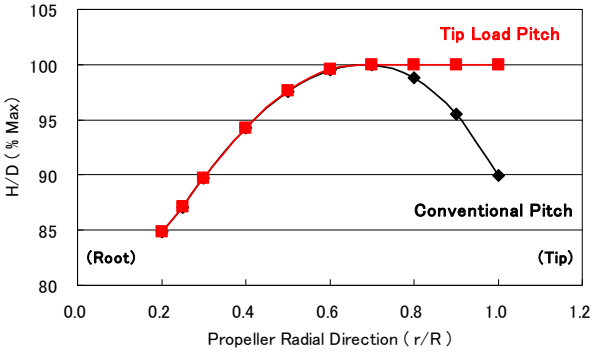

Figure 4 Propeller Pitch Distribution

Figure 5 shows the results of VLM calculations of radial thrust distributions for the 2 propellers in the bollard pull condition, clearly showing the high thrust of the tip-load type pitch-distribution propeller near the nozzle.

Figure 6 shows the results of calculations in which this thrust distribution is used as the radial distribution of body force in the two-dimensional CFD propeller model investigated in the previous section. Comparing pressure distributions at the nozzle fore part confirmed higher negative pressures with the tip-loaded pitch propeller. We achieved improvements of approximately 1.0% for KTT/10KQ, an indicator of propeller efficiency of the bollard pull condition. KQ and KTT are defined respectively by equation (3) and (4).

$$KQ = \frac{Q}{\rho \cdot n^2 \cdot D^5} \tag{3}$$

$$KTT = KTP + KTD \tag{4}$$

Where KQ = propeller torque coefficient; Q = propeller torque; KTT = total thrust coefficient; ρ = density of water; n = propeller revolution number; D = propeller diameter.

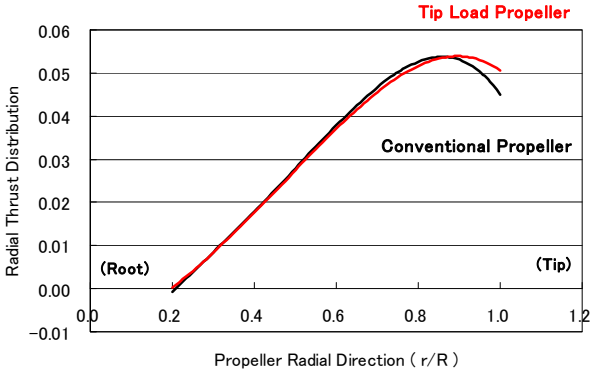

Figure 5 Radial Propeller Thrust Distribution

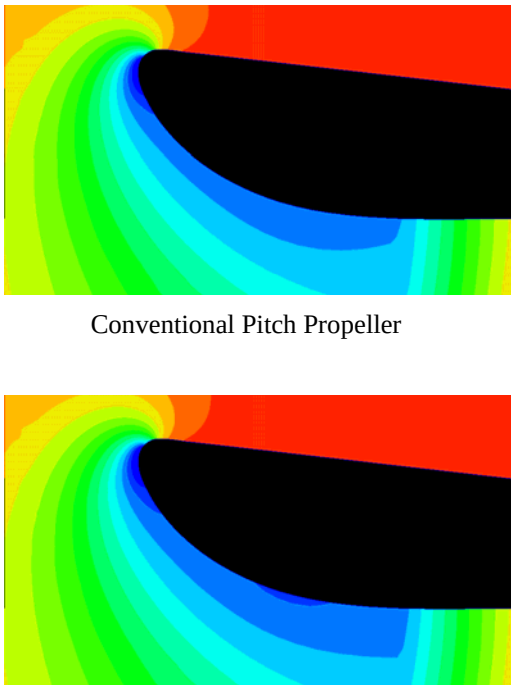

Conventional Pitch Propeller

Tip Loded Pitch Propeller

Figure 6 Comparison of Pressure Distribution with Propeller Tip Load

2.3 Interaction between the nozzle and the propeller

The effects of propeller pitch distributions affected inflow velocity into the nozzle were studied. Next the geometric composition of the nozzle and the propeller was investigated for another issue in this study. In ducted

propellers, the clearance between the propeller tip and the straight section inside the nozzle affects performance significantly. If the position of the propeller tip deviates from the straight section inside the nozzle, performance declines. We investigated the effects of the clearance between the propeller and the nozzle using a three-dimensional CFD model that considered the geometric shape of the propeller correctly. For this aspect of our study, we combined the newly-developed nozzle with a tip-loaded pitch propeller. For CFD calculation, the propeller was arranged at ±10% position of the nozzle length toward axial direction from the nozzle center so that the propeller tip deviated from the straight section inside the nozzle. We used the STAR-CD multi-reference frame (MRF) function for analysis, performing calculations for a single propeller blade to which the cyclic boundary condition was adopted. The generated meshes for 3D Analysis are show in Figure 7. The calculation conditions are shown in Table 3.

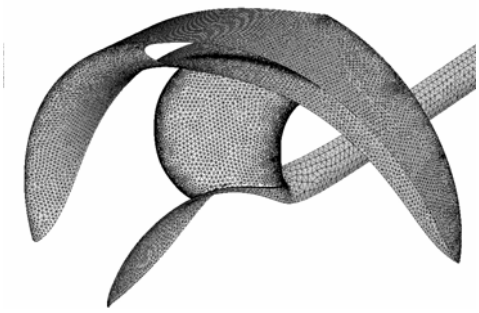

Figure 7 1/4 Cyclic Model for 3D Analysis

Table 3 Calculation Condition for 3D Analysis

Analysis Solution	3D Steady-State SIMPLE method
Discrete Scheme	QUICK
Turbulence Model	k-ω SST High-Reynolds Number model
Reynolds number	Rn = 6×10^5
Generated meshes	Approx. 1,700,000 cells (non-structured mesh)

Figure 8 shows the results of velocity distributions inside the nozzle and propeller surface pressure distributions in the bollard pull condition. Figure 9 shows the ducted propeller characteristics versus propeller tip position. Positioning the propeller forward accelerates inflow velocity along the nozzle leading edge, and increases negative pressure at the nozzle fore part and nozzle thrust. However, it also accelerates flow inside the nozzle, reducing the propeller's thrust and torque.

Positioning the propeller toward the rear weakens inflow acceleration at the nozzle fore part and reduces nozzle thrust. Additionally, since increasing the clearance between the nozzle and the propeller tip weakens flow acceleration in the propeller tip, it reduces not only propeller surface negative pressure but also propeller thrust and torque.

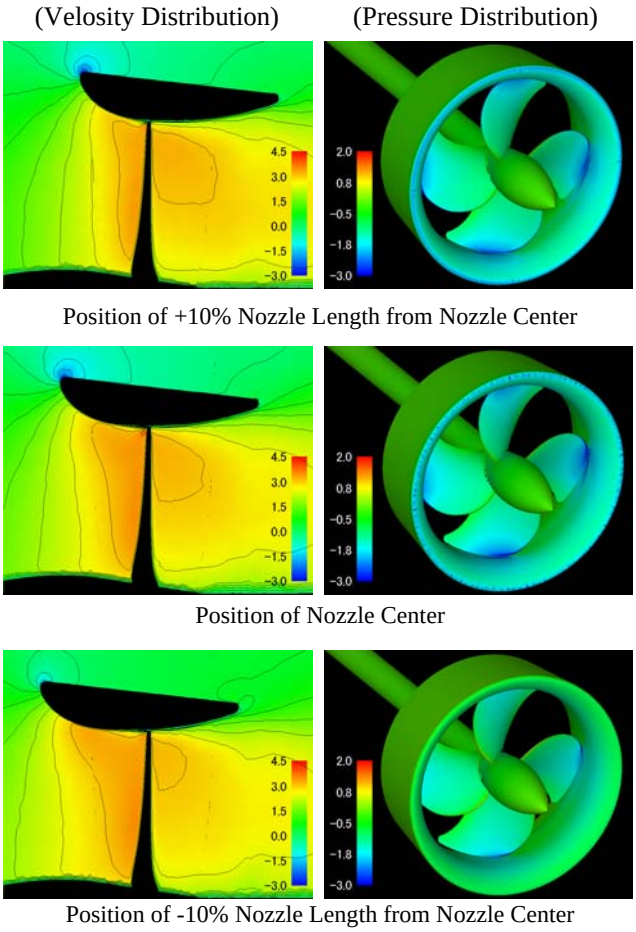

Figure 8 Comparison of Propeller Tip Position

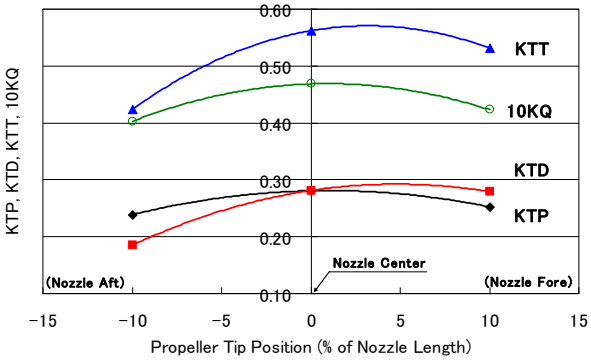

Figure 9 Calculation Results of Ducted Propeller Characteristics

Figure 10 shows KTT/10KQ values at each propeller tip position. KTT (=KTP+KTD) is a total thrust coefficient and KQ is a propeller torque coefficient. When the propeller is located toward the rear, bollard pull efficiency declines suddenly; when the propeller is located toward the front, bollard pull efficiency increases. This suggests that the optimal position for the propeller is forward of the center of the nozzle. The ideal propeller configuration maximizes interference between the nozzle and the propeller.

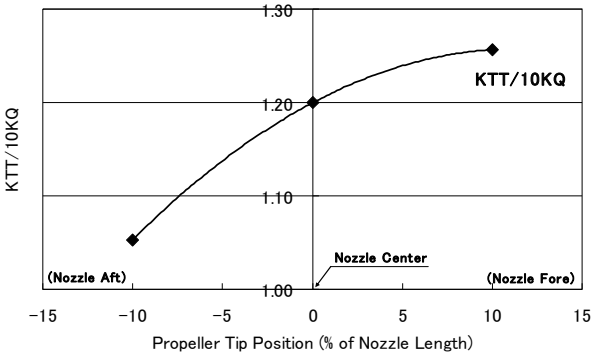

Figure 10 Calculation Results of Bollard Pull Efficiency

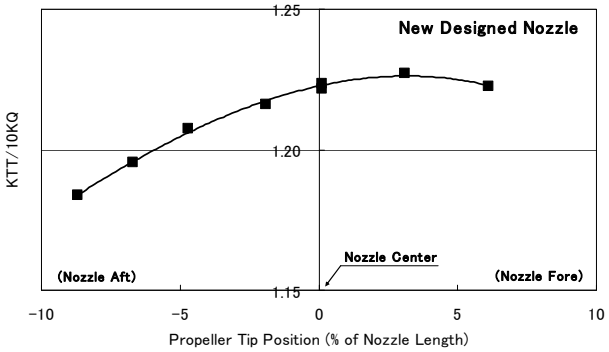

Figure 12 Model Test Results of Bollard Pull Efficiency

The next section discusses the validity of new design method by model test.

4 Model Test

To evaluate the performance of the newly designed nozzle and tip-loaded type propeller, we performed model tests using the towing tank at Akishima Laboratories (MITSUI ZOSEN) Inc. For this model propeller, we selected a mean pitch ratio that met the design conditions. Figure 11 shows the photograph of model ducted propeller.

The ducted propeller open test (POT) was carried out with a Reynolds number Rn=6x10^5. Rn is defined by equation (5).

$$Rn = \frac{n \cdot D^2}{\nu} \qquad (5)$$

Where Rn = Reynolds number; ν = kinetic viscosity; n = propeller revolution number; D = propeller diameter.

The test condition was performed with propeller rotation kept constant. Figure 12 shows the test results (bollard pull condition) when the propeller tip position is varied to confirm the effects of the relative position of the nozzle and propeller. These results show the tendency of KTT/10KQ for the position of the propeller tip and show the availability of the CFD analysis.

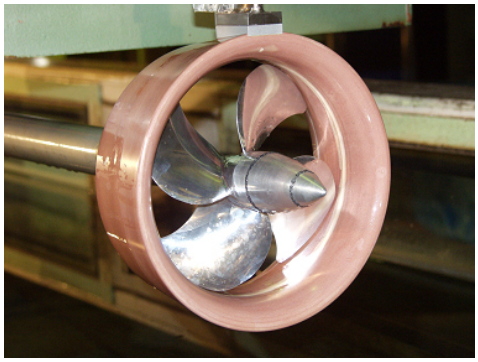

Figure 11 Model Ducted Propeller

We found that the propeller tip is 3% of the nozzle length in front of the nozzle center for the optimal propeller position. Since the center of the straight section inside the newly designed nozzle lies 47% of the nozzle length from the nozzle leading edge, this position is equal with optimal position of the propeller tip. For the new designed nozzle shape, the position of the propeller tip should be arranged on the center of the straight section inside the nozzle. When the propeller tip is at the optimal position, bollard pull thrust (twin ducted propellers) at design condition (2206 kW) is approximately 81 tons, or some 4.0% greater than the 78 tons (estimated by tank test results) provided by a conventional composition (Figure 13).

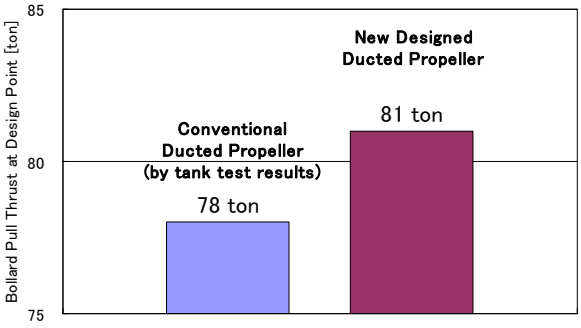

Figure 13 Comparison of Bollard Pull Thrust

5 Field Test

We also performed field bollard pull tests to evaluate the performance of new ducted propeller. Figure 14 is a photograph of the newly designed ducted propeller at full-scale dimension. The field test was carried out in Singapore. This bollard pull test was carried out for 4 ocean tugboats, each equipped with Z-pellers applying the new ducted propellers.

The results indicated a bollard pull thrust of over 80 tons (twin ducted propellers) at the design point in the ahead-pull condition. This test results demonstrated the high performance of the new ducted propeller and led to the commercial introduction of the new Z-peller.

Figure 14 New Designed Ducted Propeller at Full Scale

6 Conclusion

- To achieve over 80 tons of bollard pull thrust (twin ducted propeller), we designed a new ducted propeller based on theoretical calculation and computational fluid dynamics (CFD), and the high performance of the new designed ducted propeller was confirmed by field tests.
- To optimize the nozzle shape for higher bollard pull performance, we performed a parametric study based on theoretical calculation and CFD. The results achieved a roughly 3.0% improvement in performance for the nozzle alone, compared to the conventional 19A type.
- To increase ducted propeller performance, we introduced tip-loaded pitch propellers. With such propellers, the negative pressure at the nozzle fore part increased with a larger induced velocity. The efficiency became 1.0% greater than that of conventional ducted propellers.
- Using CFD, we also investigated the arrangement and clearance between the propeller and nozzle, finding that efficiency declined when the propeller tip was located behind the straight section inside the nozzle. We also found that locating the propeller tip forward would maximize propeller efficiency.
- We found that the relative positions of the propeller tip and the straight section inside the nozzle affected the performance of the ducted propeller.
- To evaluate the performance of new designed ducted propellers, we performed model tests and full-scale tests. The bollard pull thrust confirmed in these tests showed over 80 tons of design target and finally led to the commercial introduction of the new Z-peller model.

REFERENCES

Ishii, N. & Ide, T. (1996). 'A study on prediction of propeller slipstream and the numerical analysis of a lifting surface'. Journal of the Society of Naval Architects of Japan Vol.160.

Kawamura, T. et al. (2006). 'Simulation of Unsteady Cavitating Flow around Marine Propeller Using a RANS CFD Code'. Sixth International Symposium on Cavitation (CAV2006) Paper No.173, Wageningen, The Netherlands.

van Manen, J. D. & Oosterveld, M. W. C. (1966). 'Analysis of Ducted-Propeller Design'. The Society of Naval Architects and Marine Engineers, New York, U.S.A.

Yagi, H. et al. (1983). 'Propeller Cavitation Study of a Novel Integrated Duct Propeller System'. PRADS 83, Tokyo & Seoul.